Engineering Structures 260 (2022) 114217

Contents lists available at ScienceDirect

Engineering Structures

journal homepage: www.elsevier.com/locate/engstruct

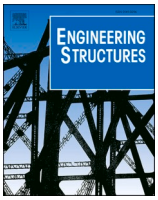

A numerical study of erosion void and corrosion effects on the performance of buried corrugated steel culverts

E. Nakhostin *, S. Kenny, S. Sivathayalan

Department of Civil and Environmental Engineering, Carleton University, 1125 Colonel By Dr, Ottawa, Ontario K1S 5B6, Canada

ARTICLE INFO

Keywords:
Corrugated Steel Culvert
Finite Element Method
Erosion Voids
Corrosion
Buried Culverts
Shallow Cover Depth

ABSTRACT

The mechanical response of a buried corrugated steel culvert, that is deteriorated due to corrosion and/or soil erosion, subject to surface loading and overburden is simulated using continuum finite element methods. The three-dimensional numerical modelling procedures were verified for culvert diameter changes using third party full-scale experimental data. The numerical simulations evaluated the mechanical response in terms of displacement, section force and moment, and equivalent plastic strain relative to the intact culvert/soil system across a range of design parameters. The sensitivity study evaluated the soil and culvert damage state as defined by the location and volume of soil erosion voids adjacent to the culvert perimeter and corrosion at invert with different angles. The mechanical response of the culvert exhibited greater sensitivity for soil erosion voids located at or above the springline with the higher potential for failure and decreased service life. The impact on the mechanical response was localized for soil erosion voids below the springline, and the culvert material can approach yield if void creation is combined with corrosion deterioration.

1. Introduction

Corrugated Steel Culverts (CSC) are core municipal infrastructure components used as part of a drainage system for watercourse and stormwater management. CSC products are thin-walled structures that have been used since the 1960 s due to their beneficial economic and technical characteristics such as strength and ductility. CSC products have a wide range of service life, from 10 to 100 years, depending on a number of factors that include geographic location, climate and CSC coatings [4]. Physical processes, related to environmental factors and ageing, can deteriorate the CSC/soil system and impair the mechanical performance and reduce the service life. Erosion voids and corrosion can develop in the backfill and CSC due to environmental conditions. The deterioration mechanisms are influenced by the presence of moisture, and soil characteristics including type, homogeneity, density, clay content and mineralogy [6,17]. The deterioration of the culvert system can result in life-threatening and expensive damage to the culverts and its related system [23].

The creation of voids within the backfill, particularly adjacent to the structure/soil interface, can influence the structure/soil interaction and load transfer processes (i.e., both stress amplitude, distribution), and failure mechanisms that may affect the stability and integrity of buried structures. Operational experience with buried structures, such as pipelines and tunnels, indicates the creation of local soil voids distributed around the structure, which can affect the structural load carrying capacity. The soil voids may be created due to water leakage through corrosion features at the base of the CSC. Hydraulic pressure and flow may washout and transport fines within the backfill leading to the creation of soil voids. Field observations have indicated that the concentration of solid particles transported with the sewage causes the formation of a groove around the pipe [7,34].

The erosion void creates a separation, or region of non-contact, between the structure and surrounding soil backfill. The presence of erosion void may result in undesirable deformation and stress within the buried structure [40]. The simulation of erosion voids can be achieved through considerations of the contact region and interaction mechanics between the structure and surrounding soil [16,39]. Local, discrete voids (i.e., separation between the structure and soil) may be introduced at different locations on the interface. Due to these changes in the contact interface, changes in the normal contact pressure were measured and the simulations indicated noticeable changes in the magnitude and distribution of earth pressure within the region experiencing loss of contact [19,36]. The presence of soil voids may reduce structural load carrying capacity, induce local soil deformation mechanisms, cause

* Corresponding author.
E-mail addresses: elham.nakhostin@carleton.ca (E. Nakhostin), shawnkenny@cunet.carleton.ca (S. Kenny), sivasivathayalan@cunet.carleton.ca (S. Sivathayalan).

https://doi.org/10.1016/j.engstruct.2022.114217
Received 13 September 2021; Received in revised form 15 February 2022; Accepted 28 March 2022
Available online 5 April 2022

eccentric loading on the structure that can lead to unexpected stresses and may cause progressive structure deterioration and failure [24,25].

Long-term atmospheric corrosion model of steel was proposed based on different atmospheric sites (i.e., rural, urban, industrial, and marine). The effect of corrosion was quantified in term of mass loss and the effect of environmental parameters considered on the corrosion rate. Large data base according to the reported information by different countries were used to establish a universal equation [15,10]. The corrosion effect of environment on steel was investigated by field observations, full-scale and laboratory tests and the steel corrosivity was classified based on data obtained in Europe and North America climate conditions [7,27,31,33].

The results from a numerical study exploring the effects of local soil voids on the structure/soil interaction mechanisms and mechanical response of a buried thin-walled CSC are presented in this paper. Three-dimensional (3D) continuum finite element models, using Abaqus/Standard software, are developed. The culvert corrugation profile is modelled with nonlinear constitutive relationships defining the CSC and soil material behavior and contact interactions at the CSC/soil interface. A single-wheel pair and single axle loads are positioned over the culvert crown at the ground surface defined the surface loading condition. Confidence in the numerical modeling procedures is established through verification with data from third-party physical modeling studies [31]. The parametric study investigates the influence of soil erosion void volume (i.e., angle, depth, length) and the relative position with respect to the culvert (i.e., distance, location), on the mechanical response of corrugated culvert buried in shallow cover depth. Shallow cover depth is defined as a normalized cover depth less than two [29]. The effects of combined erosion and corrosion is studied for two cases. The analysis includes an assessment of the culvert serviceability with respect to the sectional moment, force, strain, and displacement of CSC and the soil pressure in presence of soil voids and corrosion.

2. Numerical modelling procedures and verification

Continuum finite element modeling procedures were used to examine the mechanical response of a buried CSC subject to the applied surface loads with deteriorated backfill conditions due to soil voids at the CSC/soil interface. Based on previous studies [12,20,21,28] the corrugated profile of the culvert was modeled explicitly and incorporated within the model geometry in order to accurately predict the CSC section moment and force, particularly for shallow burial conditions. As noted previously, shallow burial condition is defined as$H/D < 2$, where H is cover depth and D is culvert diameter [29].

2.1. CSC/Soil and loading system

A 900 mm diameter CSC with a wall thickness of t mm, and corrugated profile of depth and pitch was considered in the analysis and the CSC profile and the section properties for two CSC profiles which are used in this study are presented in Fig. 1 and Table 1. In numerical modeling, the culvert section was discretized using fully integrated linear 4-node (S4) shell elements for the model space with three elements from crest to trough to have optimum mesh density.

The culvert was buried at 900 mm cover depth (H/D = 1) within a soil domain representing backfill conditions as shown in Fig. 2a. The soil box dimensions were selected based on the convergence sensitivity study and third-party experience [21,31,33], requirements for applying the surface load [9,21,33] effects on the CSC/soil response, and bedding (greater than0.5 D) thickness [13,14,22]. Eight node linear brick elements (C3D8) were used to discretize the soil domain with the boundary conditions which replicate the experimental setup. The soil domain base was fixed from motion (i.e., $U_X = U_Y = U_Z = 0$), and the sidewall vertical faces were constrained from the transverse lateral motion (i.e., $U_X = U_Y = 0$).

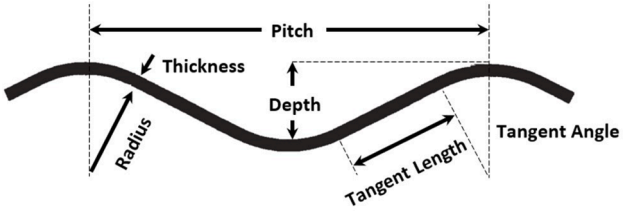

Fig. 1. Corrugated Steel Culvert (CSC) profile.

In the full-scale tests, plastic deformations were observed in the culvert for shallow cover depth for $H/D = 0.5$ [29,33]. In this numerical study, the CSC and soil constitutive relationships accounted for nonlinear material behavior. The culvert constitutive relationship was based on J2 plasticity theory with the von Mises (equivalent stress) yield criterion and combined hardening rule [18]. The stress–strain relationship was constructed using piecewise approximation based on Ramberg-Osgood expression assuming Grade A steel was representative of the coupon test data with yield strength and ultimate strength of -230 MPa and 330 MPa, respectively [32,35].

The backfill conditions were considered to be poorly-graded granular soil [1] with a unit weight of 21 kN/m3. The generation of excess pore-water pressure is not modeled in this study. This culvert is buried in granular soil and pore water can easily drain out laterally from the soil, and hence a drained analysis is considered appropriate. Generally, the water table would be below the base of this structure under normal conditions. Table 2 summarizes the mechanical properties of the two types of soils that are used in the verification study. Soil I is the main soil property that is used in parametric study of the numerical analyses. In verification procedure, Soil II is used for modeling soil from invert to crown in the numerical simulation. Modification in the reduced strength parameters (i.e., friction and dilation angle) for Soil II represents the general effects of erosion and deterioration of the backfill conditions. The defined magnitude for each parameter was based on the conducted experimental full-scale tests and some sensitivity numerical studies [13,14,22,29,31,33]. A cohesion value of 1 kPa was defined to mitigate issues with numerical convergence. The plastic response was governed by the Mohr-Coulomb failure criterion with the flow potential was defined as a hyperbolic function in the meridional stress plane and smooth elliptic function in the deviatoric stress plane. A non-associated flow rule was used in the simulation [18,26]. The adopted modified Mohr-Coulomb model is capable of simulating soil material hardening and softening behavior due to applied stresses and strains [2,18,37].

The CSC/soil backfill interface was modelled as deformable with the culvert defined as the master surface for the contact pair. Tangential interface behavior using the penalty formulation with finite sliding on the contact area is used to model CSC/soil interface [18,38].

As shown in Fig. 2b and c, the single axle and wheel pair loadings based on the Canadian code (CHBDC) is applied as a service load for the soil cover depth ($H = 900$ mm) examined in this study [5,9,11]. To apply the truck load, the load pad was modeled based on the experimental program and measured 600 mm in length and 250 mm in width [9,31].

2.2. Verification study

The validity numerical modelling procedures were verified using the horizontal and vertical diameter changes reported from full-scale experiments [31]. The diameter change of CSC is verified at total 189 kN under the single axle load at 900 mm of cover depth. The control pipe test examined the response of the corroded culvert with a 900 mm diameter and 3140 mm length of a buried culvert subject to changes in the service load conditions. The corrugated spiral profile of the control pipe had a depth of 12.5 mm, pitch of 67.7 mm, and nominal wall thickness of 3.5 mm with no deterioration effects (Profile I in Table 1). The culvert material was conventional steel grade with an elastic

Table 1
Section properties for CSC (Corrugated Steel Pipe) [8].

	Pitch (mm)	Depth (mm)	Radius (mm)	Wall Thickness, t (mm)	Tangent Length (mm)	Tangent Angle (degree)	Area (mm^2/mm)	Moment of Inertia (mm^4/mm)	Section Modulus (mm^3/mm)
Profile I	67.7	12.7	17.46	3.5	18.269	27.381	3.621	70.16	8.74
Profile II	67.7	12.7	17.46	1.6	19.578	26.734	1.512	28.37	4.02

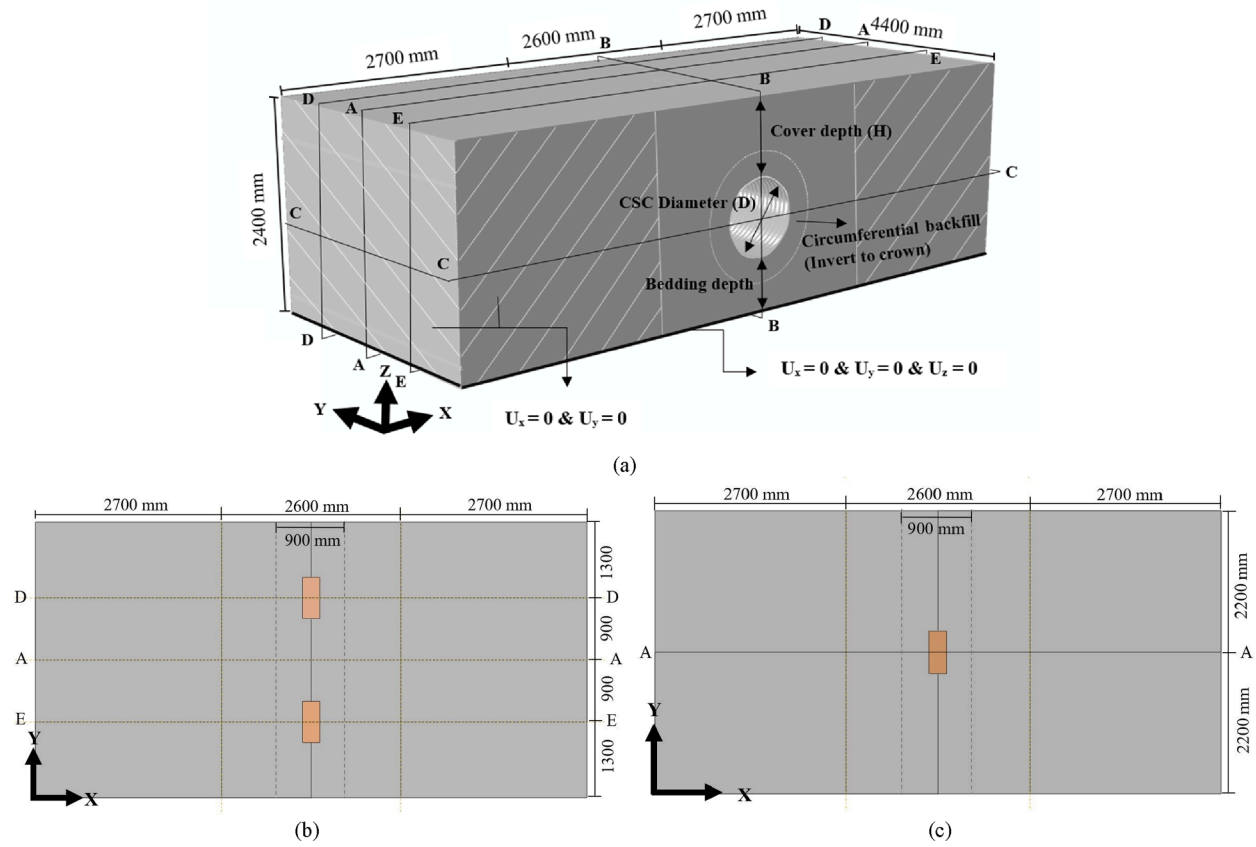

Fig. 2. a) continuum finite element model geometry for the soil backfill domain and kinematic (natural) boundary conditions, x-y plan view of b) single axle loading, and c) single wheel pair loading.

Table 2
Soil material properties.

Soil parameters	Symbol	Soil I	Soil II	Unit
Young's modulus	E	14.8	14.8	MPa
Poisson's ratio	ν	0.3	0.3	
Angle of friction	φ	43	30	deg.
Dilation angle	ψ	13	0	deg.
Cohesion	c	1	1	kPa
Unit weight	γ	21	21	kN/m^3

modulus of 200 GPa, yield strength of 230 MPa and ultimate strength of 330 MPa. The soil of bedding, invert to crown, and cover (see in Fig. 2a) were compacted to almost 88%, 87%, and 93% standard Proctor respectively and were classified as a poorly graded sandy gravel soil, "GP-SP", using the unified soil classification system. The simulated standard single axle was imposed on the ground surface and positioned over the culvert crown (Sections D-D and E-E in Fig. 2b) and was applied using the wheel pad (250 mm × 600 mm in plan) based on CHBDC for the service load conditions.

Fig. 3 presents 2D view of the verified model (control pipe) with full-scaled test results which are conducted at Queen's university. In the circumferential section of the culvert, crown is located at 12o'clock

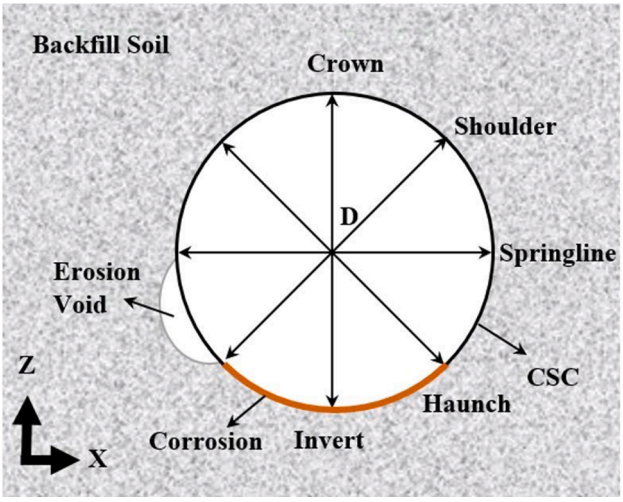

Fig. 3. 2D representation of the soil erosion void and corroded culvert for verified Control Pipe.

position, shoulders are located at 1:30 and 10:30 clock positions, springlines are located at 3 and 9o'clock positions, haunches are located at 4:30 and 7:30 clock positions and invert is located at 6o'clock position. The culvert is heavily corroded at the invert from haunch to haunch (with 15% remaining thickness in the numerical models) and the void is located on one side of the culvert/soil system from the haunch to the springline. These deteriorations are applied along the full length of the culvert/soil system [31]. The same geometrical parameters and locations of erosion void and corrosion deteriorations in the full-scale test are used in the numerical simulations. In Model 1, the material of backfill soil is Soil I, and the bedding and circumferential soil material from invert to crown is Soil II. In Model 2, the soil material for backfill, bedding, and circumferential soil is Soil I (Table 2). Fig. 4 presents X-Z view of Model 1 and Model 2. The responses of two numerical models are compared with the results of full-scaled test. The results of this verification is presented in the results section.

2.3. Soil erosion voids

Soil voids are associated with erosion mechanisms due to water flow that tend to remove fines within the backfill as a result of hydraulic/pressure gradients. The soil voids within the backfill domain are simulated as a discrete geometric feature on or near the CSC/soil interface and was modelled as a non-contact region (Fig. 5). The soil material used in these simulations are Soil I (Table 2) for all sections of backfill soil and for the culvert, Profile II is used (Table 1). The variables for modeling void geometry are presented in Fig. 5 including void angle (β), void depth (d_v), void chord length (c_v), void length (L_v), and void distance from culvert (r_v).

The soil erosion void geometry (i.e., volume) is defined by the void depth (d_v) normal to the CSC surface in the radial direction, void angle (β) prescribing the circumferential arc length subtended from the CSC longitudinal axis, and void length (L_v) parallel to the CSC longitudinal axis. The soil void position was defined relative to the CSC perimeter and centered at the crown, the left shoulder, the left springline, the left haunch, and the invert. The distance of the void edge is measured from the CSC wall edge (r_v) and the soil void erosion features are illustrated in Fig. 5, Fig. 6, and Fig. 7 as 3D and 2D graphical representations.

The soil void parameters were based on engineering judgement and consideration of field observations, experimental data, and numerical simulations [3,7,19,25,36]. The soil void was asymmetrically modelled on one-side of the CSC/soil system.

2.3.1. Parameter study of erosion void

The baseline parameters for the FE models which incorporate the soil erosion voids are summarized in Table 3. This table includes five independent parameters including the void angle (β), void depth (d_v), void length (L_v), void distance (r_v), and void location. In this analysis, void

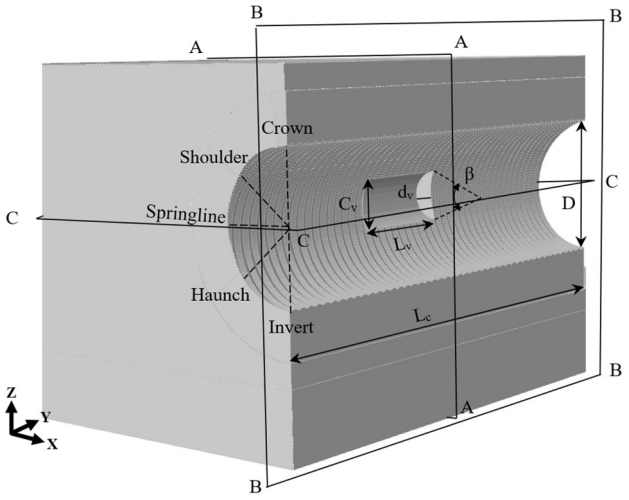

Fig. 5. 3D view of the soil erosion void characterization, cross-section B-B.

depth (d_v) normalized with void chord length (c_v), void length (L_v) normalized with culvert length (L_c), and void distance (r_v) normalized with culvert diameter (D).

A sensitivity study evaluated the influence of each parameter, while keeping all other parameters constant, on the CSC mechanical response (i.e., section force and moment) for uniform soil conditions and specific operational parameters. The sensitivity analysis (Table 4) extended the baseline parameters (Table 3) across a range to define different cases of soil erosion void size or volume (i.e., angle, depth, length) and relative position (i.e., distance from the culvert, location on the culvert perimeter). Except for the studies exploring the effects of void length on the CSC mechanical response, the numerical simulations incorporated a soil void length equal to the culvert length (i.e., $L_v/L_c = 1$). A shaded greyscale legend was defined to map the soil erosion void parameter variation (Table 4) with the graphical representations (Fig. 7). A schematic illustration of the soil erosion void position (i.e., distance, location) relative to the culvert is shown in Fig. 8. Two auxiliary studies were also conducted to evaluate the effects of a distributed soil erosion void on the culvert mechanical response (Fig. 8), which included a distributed soil erosion void extending from the culvert crown to spring line, while the other case examined a distributed soil erosion void extending from the culvert haunch to haunch.

Fig. 8 presents two models for evaluating the effect of extended soil voids. The distributed soil void examined the loss of contact due to soil void extending from the CSC crown to springline (*Case*1) and haunch to haunch (*Case*2). The Void information for these two cases is presented in Table 5. It is recognized that voids in the zone from crown to springline

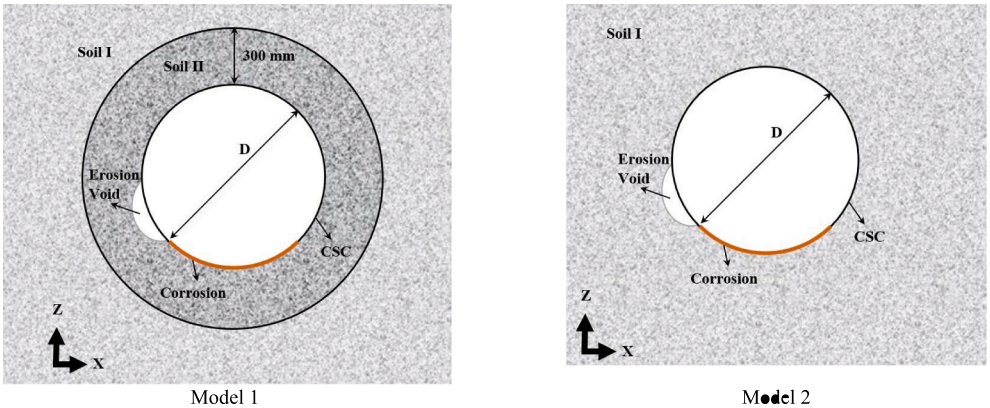

Fig. 4. 2D representation of the soil erosion void and corroded culvert for Control Pipe verified with the laboratory test conducted by the third party.

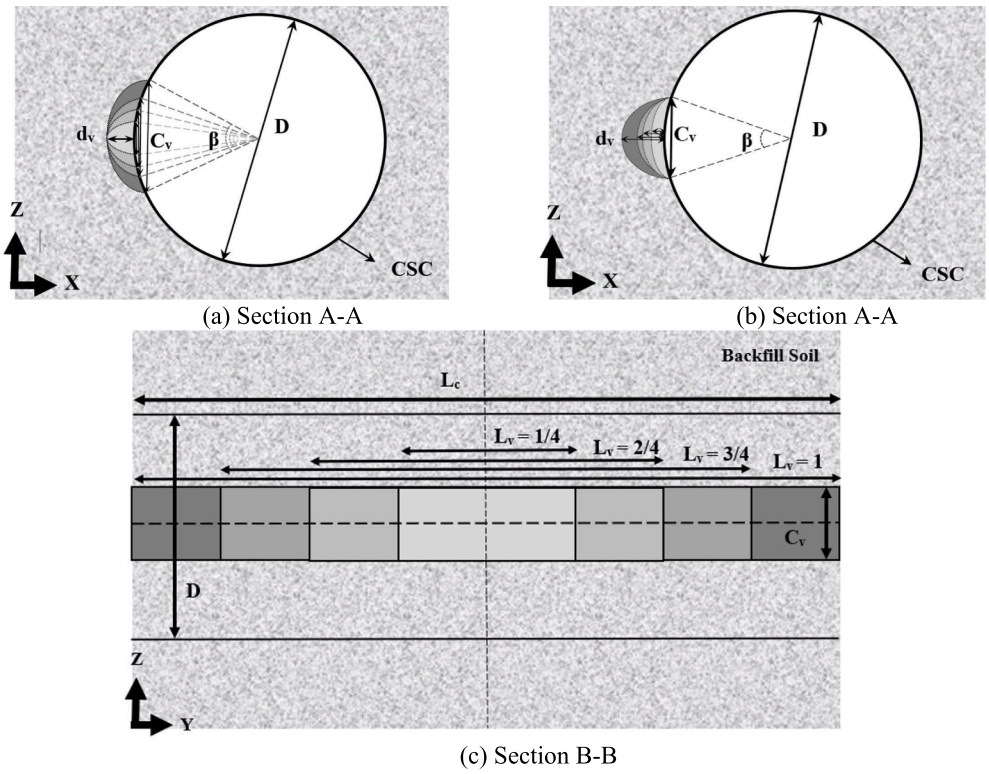

Fig. 6. 2D representation of the soil erosion volume for a change in the void a) angle (β), b) depth (d_v), and c) length (L_v).

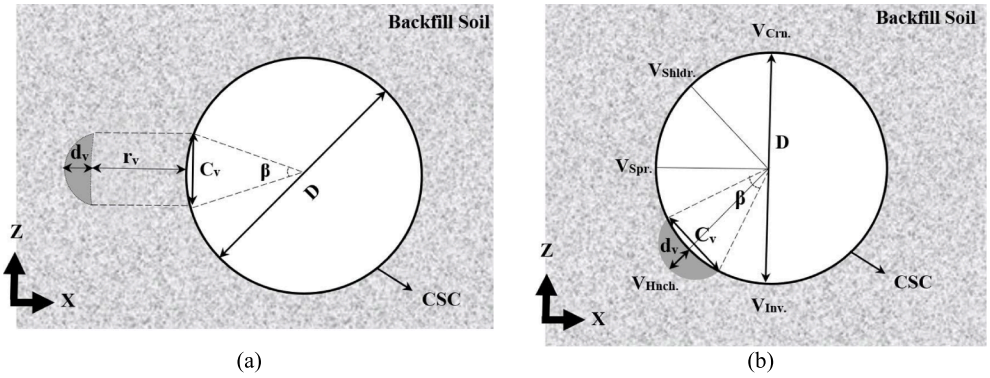

Fig. 7. 2D representation of the soil erosion void position for a change in the void a) distance (r_v), and b) location.

Table 3
Baseline eroded model for sensitivity analysis on soil void geometry and location.

Soil Void Parameters	
Void Angle, β (rad.)	$\frac{\pi}{4}$
Normalized Void Depth, d_v/c_v	0.5
Normalized Void Length,L_v/L_c	1
Normalized Void Distance,r_v/D	0
Void Location, $V_{Loc.}$	Springline

may only be transitory in-situ in granular backfills, and the analysis is intended to capture the effects of such a void geometry during the short time frame of its existence.

Table 4
Parameter range for sensitivity analysis on soil void geometry and location.

Figure Legend Color Key (Fig. 7)					
Soil Erosion Void Parameters	**Soil Erosion Void Parameter Range**				
Void Angle, β (rad.)	π/12	π/6	π/4	π/3	
Normalized Void Depth, d_v /c_v	0.3	0.4	0.5	0.6	
Normalized Void Length, L_v /L_c	1/4	2/4	3/4	1	
Normalized Void Distance, r_v /D	1	2/3	1/3	0	
Void Location, $V_{Loc.}$	Invert	Haunch	Springline	Shoulder	Crown

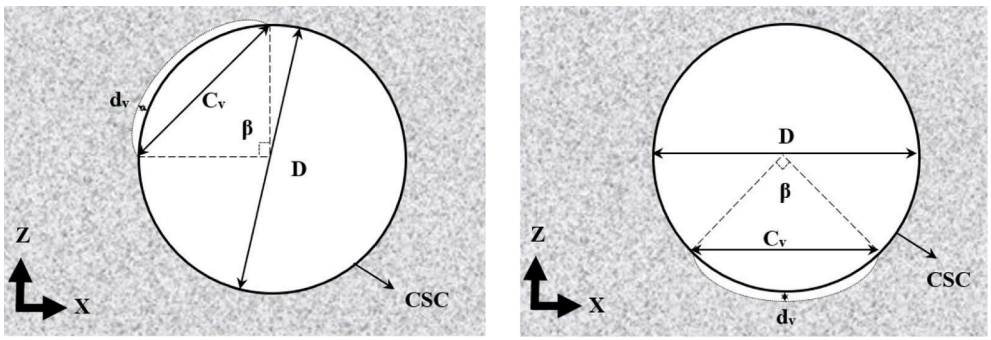

Fig. 8. 2D representation of the distributed soil erosion void extending from the culvert crown to springline, and from the haunch to haunch.

Table 5
Two particular cases of erosion voids.

Soil Void Parameters	Case 1	Case 2
Void Angle, β (rad.)	$\pi/2$	$\pi/2$
Normalized Void Depth, d_v/c_v	0.04	0.04
Normalized Void Length, L_v/L_c	1	1
Normalized Void Distance, r_v/D	0	0
Void Location, $V_{Loc.}$	Crown-Springline	Haunch-Haunch

Table 6
Two particular cases of combined erosion void & corrosion.

Culvert Corrosion Parameters	Case 1&Corrosion	Case 2&Corrosion
Corrosion Angle, θ (deg.)	$90^o and 180^o$	$45^o, 90^o, and 135^o$
Remaining Thickness (%)	34	34
Corrosion Length, $\frac{L_{cr}}{L_c}$	1	1
Corrosion Location	Invert	Invert

2.4. Combined erosion and corrosion deteriorations

Corrosion and erosion deterioration features occur in the culvert invert and surrounding soil simultaneously. The influence of combined deterioration features was examined in this study. The corrosion deteriorations are applied in internal surface of CSC located at invert with different corrosion angles (θ). The general corrosion defined at invert section with 34% remaining thickness. The corroded section length (L_{cr}) is equal to the culvert length (L_c). Two-dimensional X-Z view of culvert/soil section presented in Fig. 9 for two studied cases and Table 6 presents magnitudes of corrosion deterioration variables.

3. Results and discussion

Results are presented for each component variation of erosion void (i.e., 3 void geometries, 2 void locations, and 2 extended void profiles), combined erosion and corrosion, and effects of cover depth investigated in the parameter study. The CSC mechanical response with respect to the section force, section moment, combined force and bending moment, and soil backfill stress response is examined and compared with the intact CSC/soil system.

The circumferential results reported for the spiral path to present internal force of CSC. This spiral path is located at the mid-length of culvert around section A-A in Fig. 2a along the helical path from Invert to Invert.

3.1. Verified the numerical simulation results

Fig. 10 presents the culvert diameter change in vertical and horizontal directions for Model 1 and Model 2 obtained through numerical simulations and the laboratory test results of the full-scale experiment [31]. The numerical simulations (FEM) and the full-scale physical test results are generally consistent. Model 1 and Model 2 predicted culvert vertical diameter change with difference of −14% and 14% respectively, and horizontal diameter changes with a variation of 13% and 36% respectively. There discrepancy between the FEM result and the Full-Scale Test results was attributed to the variability in the CSC/soil loading conditions due to unloading activities, which were not accounted for during the finite element simulations.

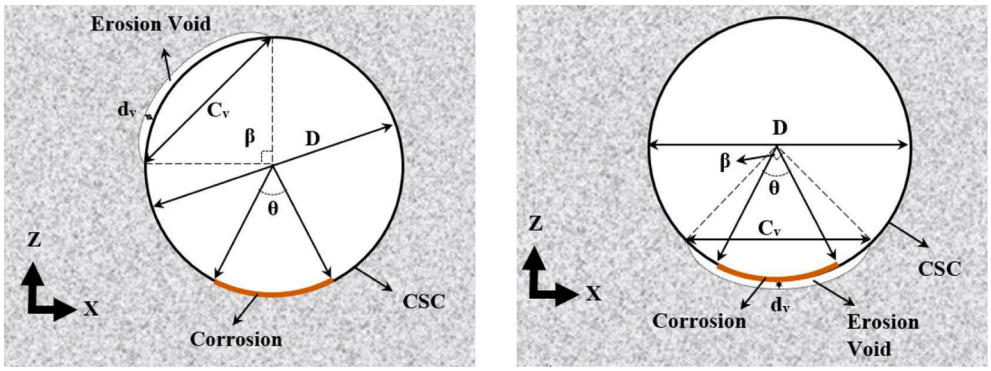

Fig. 9. 2D representation of the distributed soil erosion void and applied corrosion.

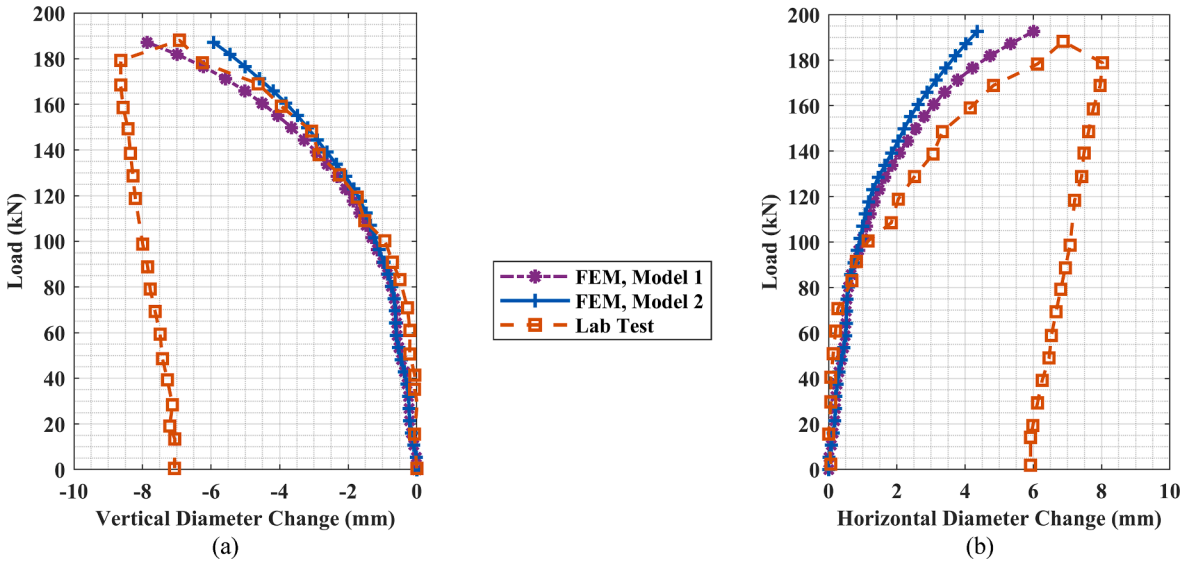

Fig. 10. a) vertical and b) horizontal diameter change of culvert under single axle loading.

3.2. Soil erosion volume effects (angle, depth, and length)

The legend "Int." in the figures presents results for intact CSC/soil structure. As shown in Fig. 11, for the intact CSC/soil system the maximum section moment and force were predicted at the pipe crown and shoulder.

Across the range of soil void erosion parameters (Table 3, Table 4) investigated, the culvert section moment and force response was effectively identical to the intact CSC/soil system response for the righthand side (i.e., crown to invert for the 12 to 6 clock positions). Due to the presence of the soil erosion voids, the predicted CSC section moment and force exhibited an asymmetric distribution that was biased on the left-hand side (i.e., clock positions 6 through 12).

Increasing the soil erosion void angle (β), depth (d_v), and length (L_v), (Fig. 11a, b, and c), increased the predicted section moment and section force with the local maximum change positioned near the springline. The soil erosion voids influenced the magnitude and mode (i.e., sense, gradient, distribution) of the CSC section moment and force response. A local maximum change of response was developed that was focused on the culvert springline (i.e., 9 clock position) relative to the intact CSC/soil system predictions. As the soil erosion void parameters increased, and reached the study range limits, the magnitudes of local maximum force and section moment at the springline (i.e., 9 clock position) equaled the peak magnitudes for the CSC/soil system response. Across the range of parameters studied, there were observed differences between the intact and perturbed system for the section moment and force response between the culvert invert (i.e., 6 clock position) and crown (i.e., 12 clock position).

For increasing void angle (Fig. 11a), the CSC section behavior exhibits a more generalized CSC response distributed between the invert and crown and tended to shift the peak magnitude response away from the CSC crown and localize at the springline with a positive section moment and negative local force. In response to the culvert section forces and deformation mechanisms, a localized response develops at culvert haunch due to the coupled interaction effects among the soil erosion void, culvert invert and bedding conditions. The soil erosion void depth and length ((Fig. 11b, c) have a localized effect at the introduced void location and there are not noticeable changes in the responses at the crown, invert, and the non-defected half of the culvert.

The spiral path distribution of the culvert section moment and local force response indicates, across the range of parameters investigated, that the soil erosion void angle had the greatest influence on the culvert's mechanical response. This observation is further explored in Fig. 12, which presents the variation of normalized internal forces (i.e., normalized section moments and forces) as a function of the soil erosion void volume parameters (i.e., angle, depth, and length). The culvert internal forces are normalized with the intact system response where the data is sampled at the culvert springline. Across the range of parameters investigated, a nonlinear response was observed and, for a specific sensitivity parameter, the relative change on section forces was the effectively the same magnitude. The soil void angle (β) exhibited a quadratic influence on the normalized section forces with a maximum (effective) multiplier value of 4. This indicates the internal forces (bending moment and local force) at the springline are approximately 4 times greater than the intact CSC/soil system response. The soil erosion void depth (d_v) and length (L_v) initially exhibited a step change in the normalized section forces (multiplier of 2) with a relatively lower gradient and maximum multiplier of 3.

Fig. 13a shows the culvert horizontal displacement at the circumferential spiral path (Displacement UX in the X-Z plane) and Fig. 13b shows the culvert horizontal displacement at the springline in longitudinal direction (Displacement UY in the X-Y plane) for soil voids with different lengths. The horizontal culvert displacement profile is consistent with the internal force response. The culvert with longest soil erosion void length (equal to the culvert length) experienced the greatest horizontal displacement at the void location and the intact CSC/soil model has the smallest horizontal displacement. All void length cases follow the similar pattern of displacement with maximum value at the mid-length and minimum values at the far ends of culvert length. The voids with finite length have localized effect on the CSC displacement in longitudinal direction and culvert section has a greater horizontal displacement at void location, while other lengths of the culvert that has soil support approach the intact culvert horizontal displacement. The normalized length of soil erosion void equal to Â¼ in Fig. 13 is consistent with the observed step change in Fig. 12 where the discontinuity enforces tighter curvature and increases section forces. Continued increasing void length results in greater flexibility and deflection with increased section forces. The reported displacement values are for three-meter length of the culvert and these values reach to zero at the two far ends of the boundary conditions.

3.3. Relative position of soil erosion void (distance and location)

Two void position variables, void distance and circumferential location, are introduced as the independent parameters to study void location effects on the CSC/soil system responses. Fig. 8a and Table 4

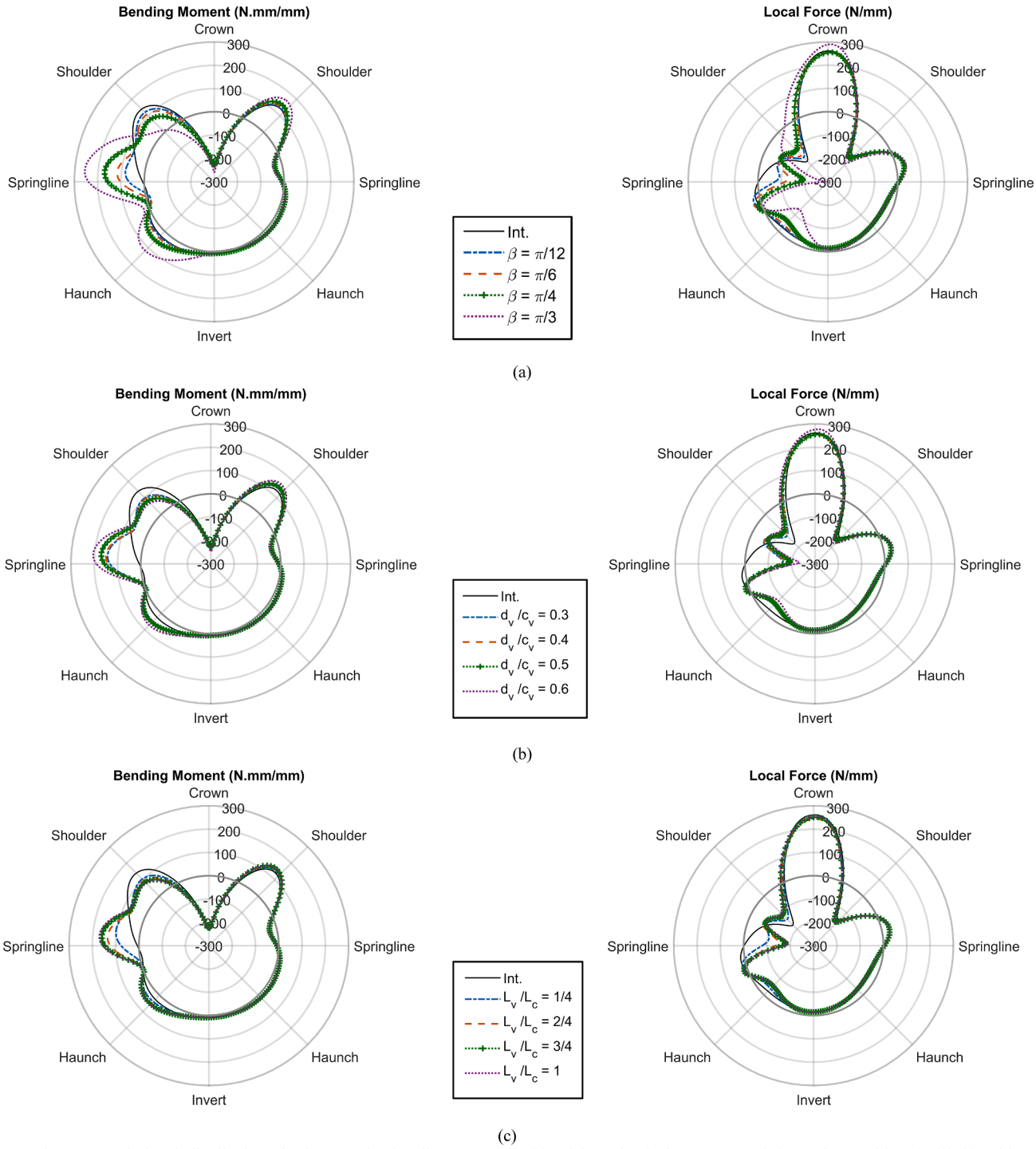

Fig. 11. Spiral path distribution of culvert section bending moment and local force for the intact case and change in a) void angle (β), b) void depth (d_v), and c) void length (L_v).

present two-dimensional view of the introduced erosion void at the springline with nonzero distance from culvert wall edge and the assigned values for each parameter related to the void position. The normalized void distance from the CSC wall edge, is the only parameter that is changing for each model. The void distance is normalized with the culvert diameter (r_v/D) which is distance of void edge from CSC wall edge as shown in Fig. 8a with assigned values equal to 1, 2/3, 1/3, and 0 mm/mm distance.

Based on the literature, circumferential location of void is a critical variable [24,25,30] and its effects on the CSC/soil responses are investigated in this numerical study. Two-dimensional view of the located erosion void at the haunch as an example of void location and the assigned values for each parameter related to the void size and position are presented in Fig. 8b and Table 4 respectively. Five different circumferential locations are assigned as the void location (i.e., Crown, Shoulder, Springline, Haunch, and Invert).

As shown in Fig. 14a, decreasing soil erosion distance (r_v) increases the predicted section moment and force with the local maximum change near the void location (springline) with greater impact for the model with zero distance ($r_v/D = 0$). The normalized void distance greater

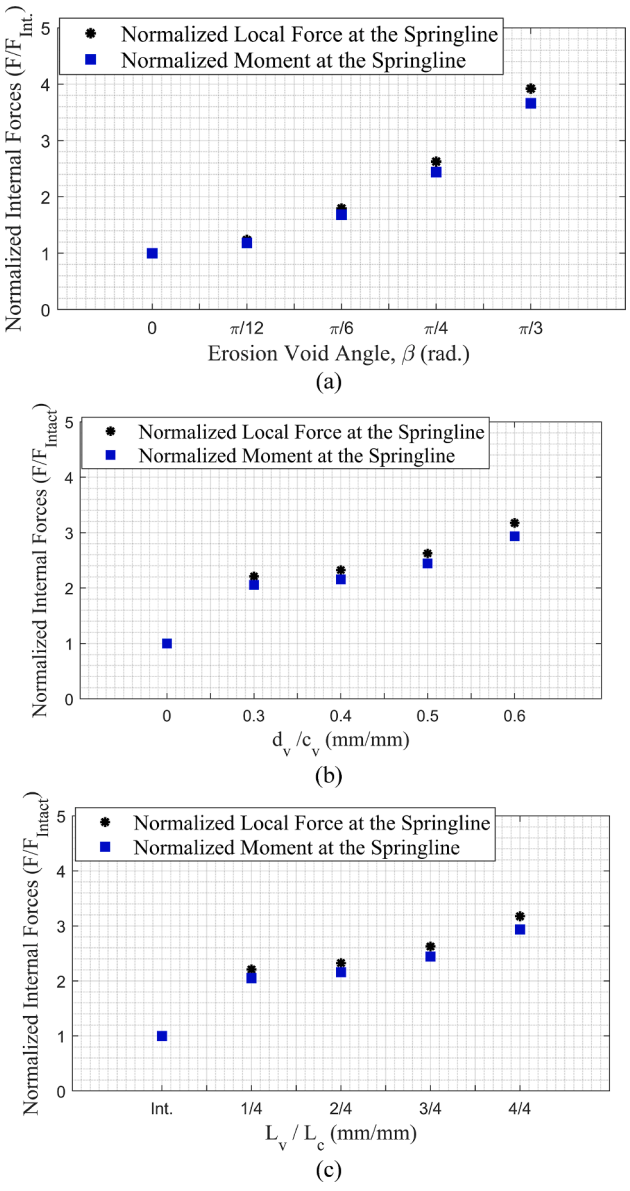

Fig. 12. Effect of soil erosion void volume on the culvert internal forces, at the springline, normalized with the intact CSC/soil response for a change in the void a) angle (β), b) depth (d_v), c) length (L_v).

than 1/3 do not have a noticeable impact on the culvert mechanical response which is almost equal to the intact CSC/soil responses and the CSC section moment and force responses are effectively identical throughout the non-defected half of the circumference.

The circumferential internal forces of the CSC due to the applied voids in the backfill soil at different circumferential locations are presented in Fig. 14b. Erosion voids located at the invert and haunch have a small local impact on the culvert mechanical response ($V_{Inv.}$ and $V_{Hnch.}$). The presence of soil voids at springline ($V_{Spr.}$) has more generalized impact on the responses. The presence of soil voids at shoulder ($V_{Shldr.}$) influence the magnitude of the section force and moment response for the CSC over practically the entire circumference. The maximum internal forces in the intact system occur at the crown and shoulder and a small change in the responses at these areas cause a noticeable change in CSC performance. Void located at the shoulder ($V_{Shldr.}$) causes increasing internal forces at the crown and shoulder and the culvert experiences yield at the crown and shoulder for the applied service load recommended in the Canadian code. Local force has a greater portion in the appearance of this behavior in comparison with the bending moment. The local force achieves the maximum capacity of the section for axial forces within the linear-elastic phase of material (Fig. 14b). These results indicate that the void location has a significant influence on the development of undesirable deformation and stress concentration. This changes the failure mechanism for shallow cover depth which is sensitive to the deterioration conditions. The presence of soil voids at crown ($V_{Crn.}$) influence the mode (i.e., direction, distribution) of the section moment and force response for the CSC. The maximum local force and bending moment for the intact system are located at crown which is transferring the surface load to the culvert. Loss of contact between the backfill soil and culvert affects load transferring mechanisms and culvert experiences lower internal forces all over the CSC in comparison with the intact system (Fig. 14b).

Fig. 15 presents the variation of normalized internal forces (i.e., normalized section moments and forces) as a function of the soil erosion void position parameters (i.e., distance, and location). The normalized internal forces of CSC increase at the springline by decreasing the void distance from the CSC (Fig. 15a). The soil void distance (r_v) exhibited a quadratic influence on the normalized section forces with a maximum multiplier value of 2.5. This indicates the internal forces (bending moment and local force) at the springline are approximately 2.5 times greater than the intact CSC/soil system response. The significance of the location effect is illustrated in Fig. 15b. The presence of soil voids at the CSC springline ($V_{Spr.}$) results in a localized increment of the CSC response at the springline (void location) with magnitude equal to 2.6 greater than the internal forces of intact system. Erosion void located at the shoulder increases internal responses at shoulder about 1.6 times in comparison with the intact system.

Void located at the shoulder causes increasing internal forces at the crown. The maximum internal forces for the intact and deteriorated systems happen at the crown and shoulder and a small change in the responses of this area causes a noticeable change in CSC performance. Fig. 15c presents the maximum value of internal forces and the culvert maximum force is almost constant for introduced voids from invert to springline. For void location at shoulder, there are increase in responses about 1.3 times and the culvert experiences plastic strain at the crown and shoulder for the applied service load recommended in the Canadian code (see Fig. 18). The soil voids located on the CSC crown appears to have greater relative influence on the CSC mechanical response. The maximum section force and bending moment for the intact system are located at crown which is transferring the surface load to the culvert. Loss of contact between the backfill soil and culvert affects the load transfer mechanisms and culvert experiences lower internal forces all over the CSC and there are decrease in internal responses about 0.4 times in comparison with the intact system (Fig. 15c).

Fig. 16 presents circumferential horizontal displacement of CSC (displacement UX in the X-Z plane).The dominant mode of this displacement is heart shaped for the intact CSC/soil system. Maximum horizontal displacement happens for the case with a void at springline and this model has high potential for horizontal displacements, and the internal forces increase accordingly. The model with soil voids at shoulder ($V_{Shldr.}$) leads to plastic strain at crown and shoulder. This result indicates that the shoulder is a very sensitive location to have a defect and presence of soil voids at shoulder influences the magnitude of the displacement and leads to creation of the plastic hinges at the shoulder and crown. Presence of soil voids at crown influences the mode of the displacement response for the CSC. The surface load transferring mechanism from ground surface to the culvert is changed and culvert experiences lower displacement, especially at the crown of the CSC in comparison with the intact system.

3.4. Extended distribution of soil erosion voids

Two special cases have been studied in this numerical modeling which place more emphasis on erosion void location with a noticeable non-contact region between soil and CSC. In these special cases, erosion

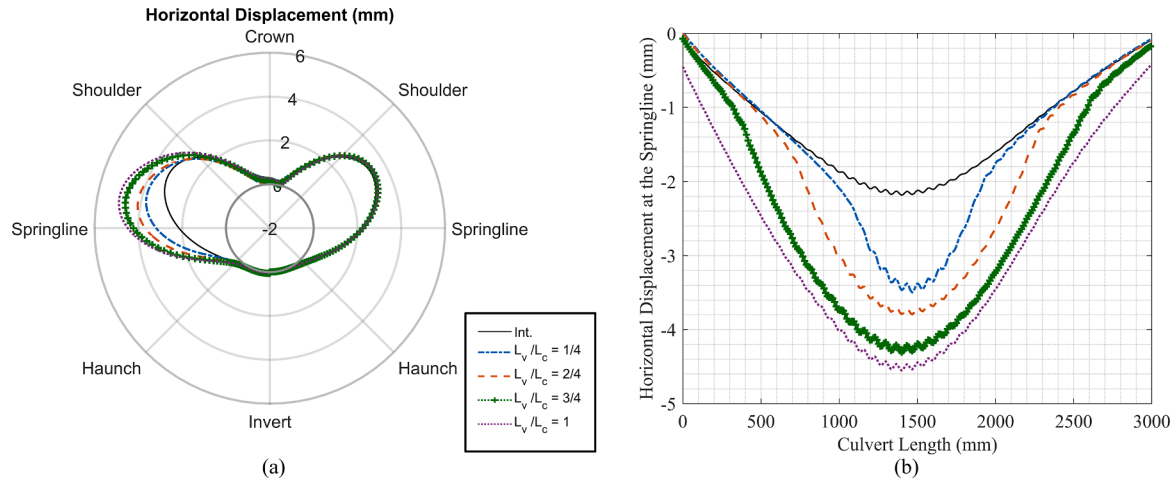

Fig. 13. Horizontal displacement of culvert at a) circumference in the spiral path and b) at springline in longitudinal direction, section C-C.

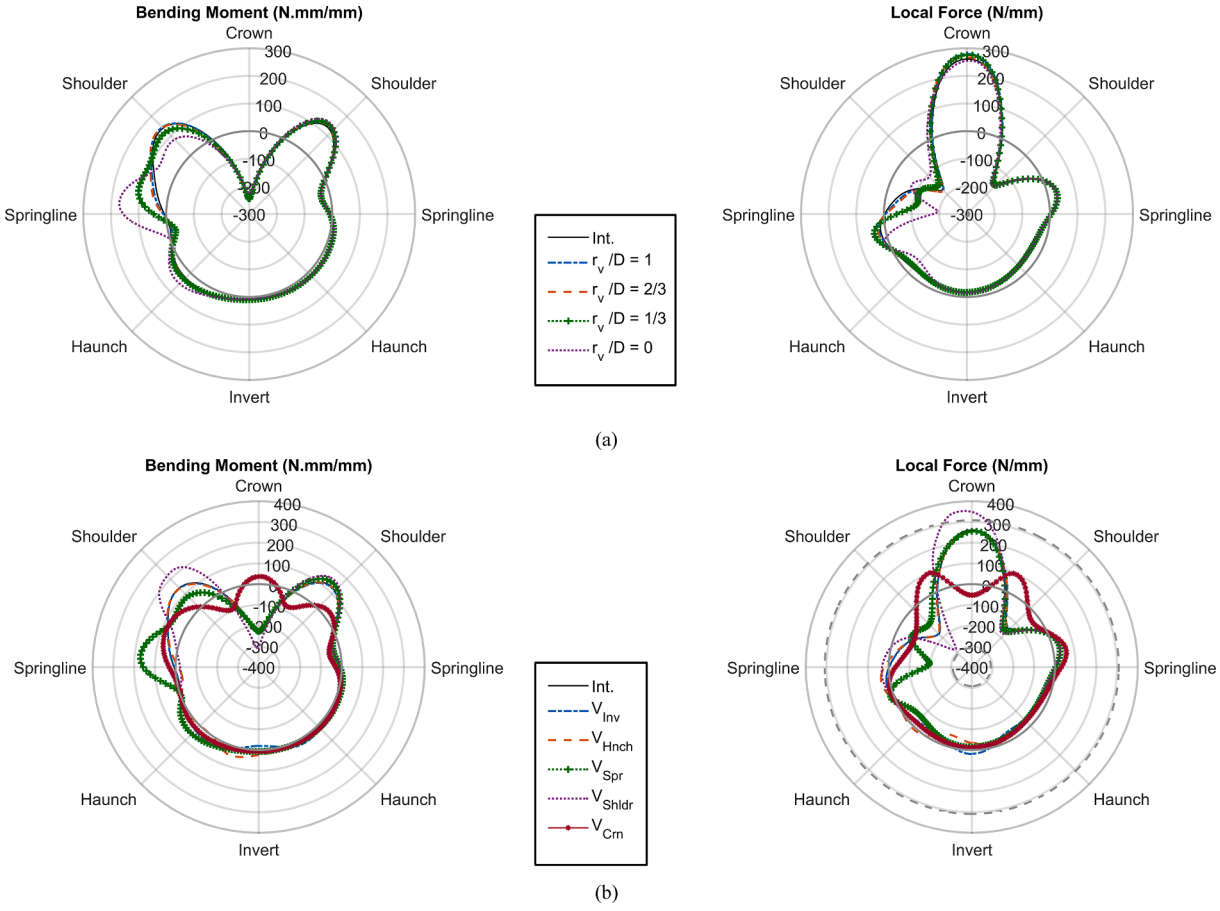

Fig. 14. Spiral path distribution of CSC section bending moment and local force for erosion voids introduced in the backfill soil with changing a) void distance (r_v), and b) void location.

void angle is equal to π/2 with a very limited normalized depth of 0.04, and full-length void as presented in Table 5. Based on the literature review and the current results, the circumferential location of void is specified from crown to shoulder for *Case*1 to represent the contact loss condition in the upper half of the CSC/soil system. The second special case (i.e., *Case*2) simulates the contact loss in the lower half of the CSC/soil system from haunch to haunch (Fig. 9).

The magnitude and distribution of the CSC section bending moment and force along the spiral path is presented in Fig. 17. In comparison with the intact CSC/soil system response, the soil void introduced in *Case*1 influenced the predicted section moment and force, particularly in the upper half of the CSC. The culvert experiences yield at the crown and shoulder for the applied service load and section force, in comparison with the bending moment, has a greater portion in appearance of yield stress (Fig. 17b). The results presented for *Case*1 indicates that losing the contact between CSC and soil can cause stress concentration which can lead to failure while the upper half of the CSC/soil system is very sensitive to the deterioration conditions. *Case*2 presents more localized

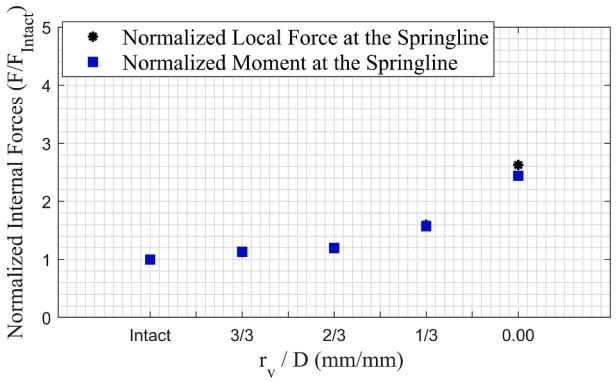

(a)

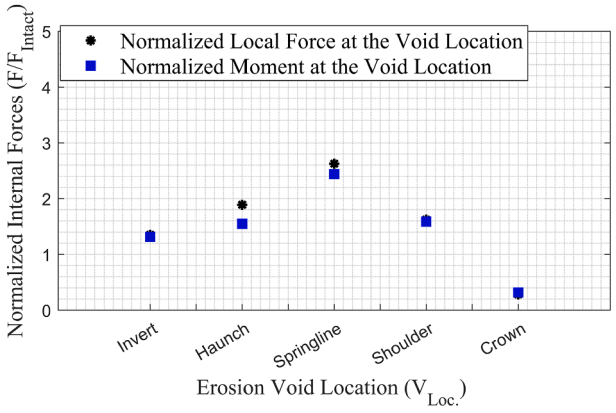

(b)

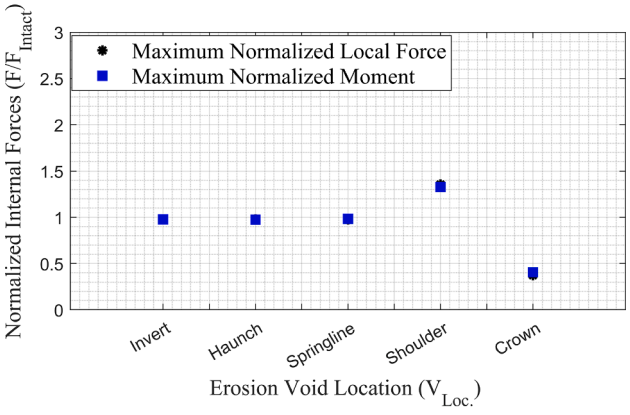

(c)

Fig. 15. Effect of the soil erosion void relative position on the culvert internal forces, at the springline, normalized with the intact CSC/soil response for a change in a) distance (r_v), b) location, and c) maximum internal forces.

effects in the internal responses of CSC. The culvert experiences small increase of section force and bending moments at invert and haunches. These results show a noticeable contact loss in the lower half of the culvert does not have a significant effect on the general performance of the culvert/soil system.

The results of numerical study and experimental tests show the maximum internal force and moment happens at crown and shoulders. The magnitude of local force is very close to the yield value and a small increase in these internal forces will lead to creation of plastic strains

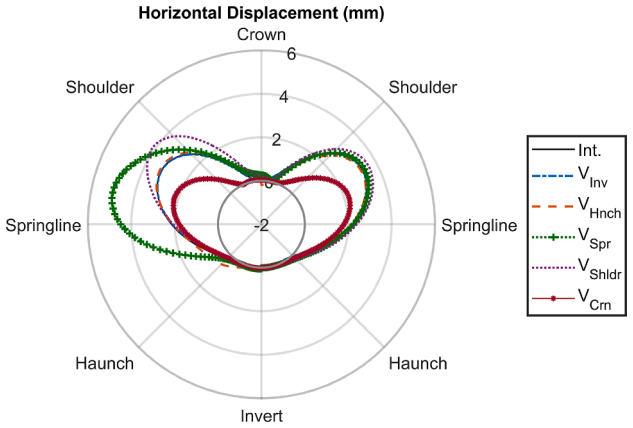

Fig. 16. Horizontal displacement of CSC in the spiral path for erosion voids introduced in the backfill soil with changing void location.

(see Fig. 14b and Fig. 17b). In this numerical study, two models experience the plastic strain at crown and shoulder that is presented in Fig. 18. Both models, ($V_{Shldr.}$ and *Case*1), experience creation of voids in shoulder and crown. Crown and shoulders are very sensitive locations and void creation in these locations places the whole system in a weak position. These results show the importance of having non-deteriorated system at upper half of the culvert.

Fig. 19 presents the changes in the circumferential soil pressure with 300 mm distance from the culvert considering the effect of erosion void. The maximum pressure for the intact structure in the reported section is located at the crown and it approaches zero at lower half following to the invert. The presence of soil voids in the upper half of backfill for these modeling sets results in a localized soil pressure response at the void location (V_{Spr} and V_{Shldr} in Fig. 19a, and *Case*1 in Fig. 19b). Erosion void located at the crown in Fig. 19a (V_{Crn}) has a noticeable impact on the surface load distribution and soil pressure and the location of maximum pressure is transferred from crown to somewhere between crown and shoulders. This model influences the magnitude and mode of the circumferential pressure for the backfill soil over the entire circumference. This result indicates the presence of voids can affect the transfer mechanism of surface loads from ground level to CSC.

3.5. Combined erosion and corrosion deteriorations

Section local force is the dominant force in the soil-culvert structure with shallow corrugated steel plate based on the Canadian code assumption, and the code recommends considering flexural effects in deep corrugated plates. The corrugated plate used in culvert modeling in this study is classified as shallow corrugated plate (pitch $<$ 380 mm, and depth $<$ 140 mm), but to meet research purposes, the combined effect of erosion void and corrosion is considered for two models of eroded soil (*Case*1 and *Case*2). The corrosion deteriorations for both cases are applied at the invert with 34% remaining culvert thickness. Fig. 20a, presents the circumferential values of $Y = \left[\frac{T}{P_{pf}}\right]^2 + \left|\frac{M}{M_{pf}}\right|$ where T and M are maximum section force and bending moment due to dead and live loads calculated using FE simulations, P_{pf} is compressive strength of a corrugated culvert section, and M_{pf} is moment capacity of a corrugated culvert section [9]. The Y value is reported for the spiral path under the wheel load section for Intact model (non-deteriorated culvert-soil system), model *Case*1 deteriorated by erosion (erosion void from crown to springline at the left side), and model *Case*1 for erosion plus corrosion with angles equal to 90° and 180°. The results indicate that circumferential Y is approaching a value equal to one at springline and shoulder in the left side deteriorated by erosion void and this value is greater than one at the crown. Applying corrosion deterioration at invert (e.g., *Case*1&θ = 190· and *Case*1&θ = 180·) does not have significant effect in

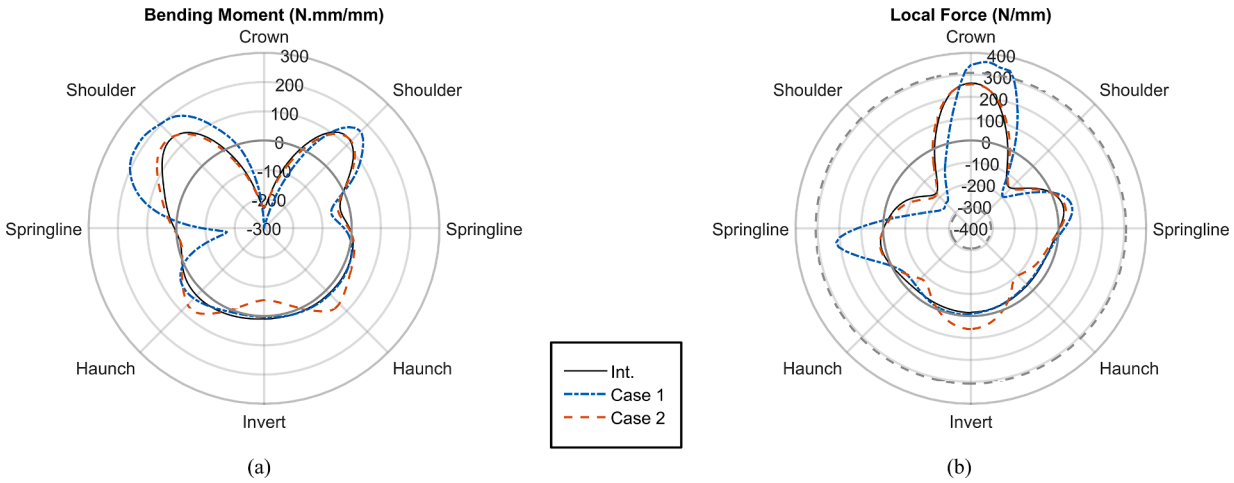

Fig. 17. Spiral path distribution of the a) bending moment and b) local force due to an extended soil erosion void.

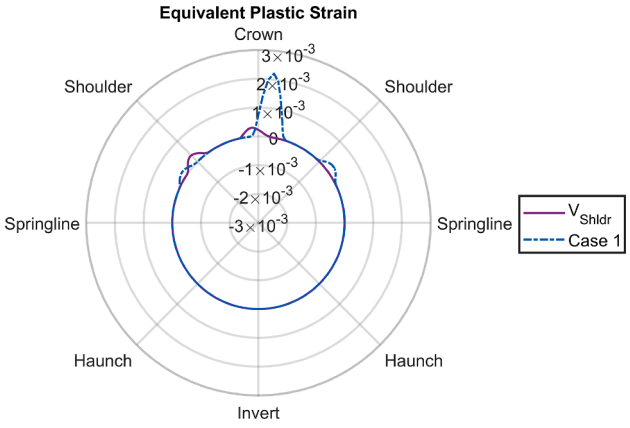

Fig. 18. Equivalent plastic strain in the spiral path.

the responses.

Fig. 20b presents the circumferential values of *Y* for the Intact model (non-deteriorated culvert-soil system), model *Case*2 deteriorated by erosion (erosion void from haunch to haunch), and model *Case*2 for erosion plus corrosion with angles equal to 45°, 90° and 135°. The results indicate that having only erosion voids at the lower half of the culvert does not have significant effect on responses and Y value remains close to zero. Further the concurrent presence of corrosion and erosion voids affects load and moment carrying capacity with respect to the reduction in the culvert thickness and this changes the load distribution. However, having only erosion void (e.g., *Case*2) at lower half of the culvert, which experiences smaller internal forces in comparison with upper half, does not have a significant effect in the general behaviour of the buried culvert. But the culvert experiences severe increase in Y responses for the cases where both erosion void and corrosion are applied at the same location. These results show that the appearance of both deteriorations in the lower half can increase the possibility of culvert failure in the lower half remarkably.

4. Summary and conclusions

The effect of soil erosion voids on the soil pressure and the mechanical response of the CSC subject to overburden and surface load was examined using continuum finite element modelling procedures. Stress concentration effects were evaluated across a range of erosion void parameters (i.e., angle, depth, length, location, proximity). The stress concentration was defined as the normalized ratio of the predicted culvert local force or moment, in response to the soil erosion void, relative to the intact culvert/soil system response.

The study of void angle and void depth indicates that the loss of surface contact and support between the culvert and surrounding soil in the upper half of the culvert/soil structure is the key contributing factor to load transfer and deformation mechanisms. The influential aspect in the void size is contact surface (void angle) and void depth does not play an important role because the culvert diameter change for this flexible case is in an order of 10 mm. The loss of surface contact is the parameter

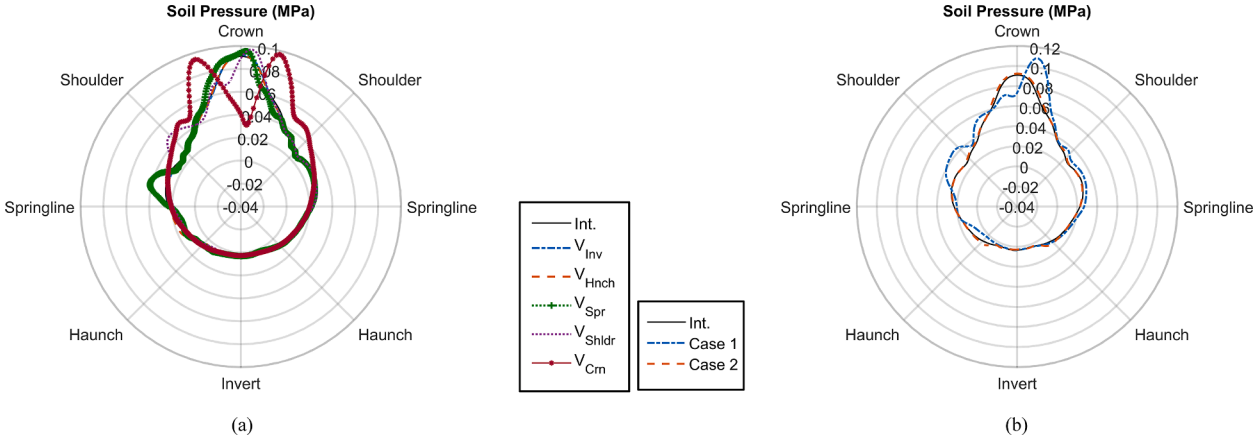

Fig. 19. Effect of losing contact between soil and culvert due to erosion voids on the changes in soil pressure.

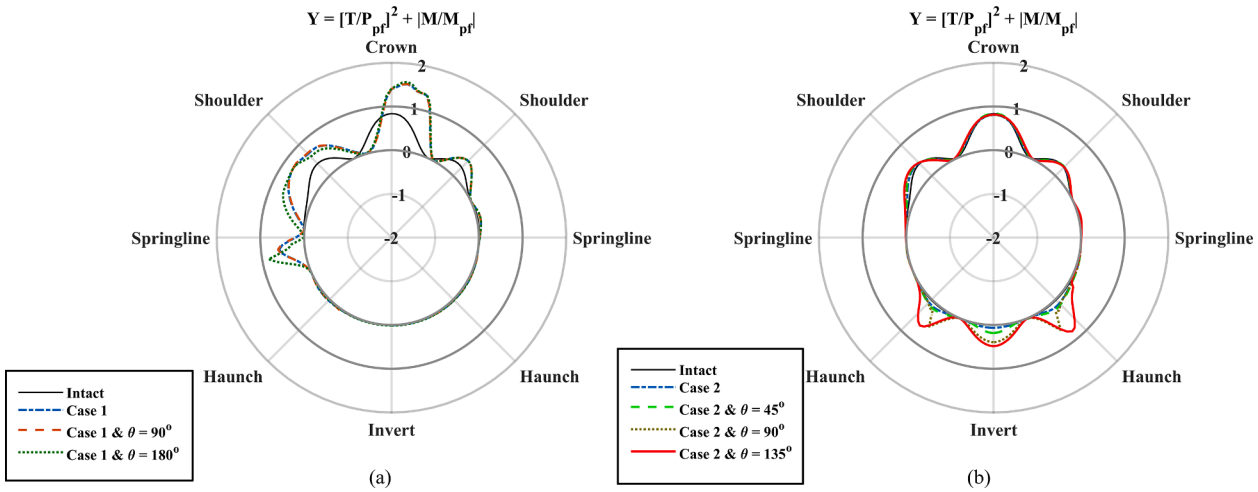

Fig. 20. Magnitude of $Y = \left[\frac{T}{P_{pf}}\right]^2 + \left|\frac{M}{M_{pf}}\right|$ for CSC for the spiral path, at the culvert mid-length for applied erosion and corrosion deteriorations a)*Case*1&*Corrosion*, and b).*Case*2&*Corrosion*

that can affect culvert performance and integrity. These outcomes may support the development of mitigation strategies for maintaining the serviceability of culvert systems and support decision making for sustainability solutions.

Based on the study of the void distance variable, the results indicate that applied void in the backfill soil with high soil pressure, where it transfers the truck load, affects the CSC results; voids located outside of this area has little to no effect in the CSC/soil system responses.

For all analysis cases, the maximum section force and bending moment occurred in the upper half of the culvert section between the springlines and responses are more severe in comparison with the lower half. The voids located in the upper half of the culvert have more noticeable effects in the load transferring mechanism and internal force responses for deteriorated systems deteriorated with erosion voids. In the model with introduced void in the shoulder, the culvert was experienced the plastic strains in the crown and shoulder due to the applied loads. This change in the performance affects the local force and bending moment distribution in the culvert.

The internal force responses do not change due to the introduced erosion voids in the lower half of culvert/soil system. But this system approaches yield point at invert and haunches when erosion void is combined with corrosion deterioration at the invert. Invert, haunch, shoulder, and crown of circumferential area is approaching the yield stress for cases deteriorated by combined erosion void and corrosion in lower half due to local force and bending moment in this structural system, but the section force is the influential internal force in comparison with the bending moment. This can cause undesirable deformation, stress concentration and eventually failure of load-carrying system for the shallow cover depth cases.

CRediT authorship contribution statement

E. Nakhostin: Conceptualization, Methodology, Software, Validation, Formal analysis, Investigation, Resources, Writing – original draft, Visualization. **S. Kenny:** Conceptualization, Software, Validation, Formal analysis, Supervision, Project administration, Funding acquisition. **S. Sivathayalan:** Validation, Formal analysis, Supervision, Funding acquisition.

Declaration of Competing Interest

The authors declare that they have no known competing financial interests or personal relationships that could have appeared to influence the work reported in this paper.

Acknowledgments

This study was conducted as a part of a doctoral research program conducted by the candidate Elham Nakhostin. The authors would like to acknowledge financial assistance from the NSERC Discovery Grant, and Carleton University.

References

[1] ASTM, D2487-11, 2011. Standard practice for classification of soils for engineering purposes (Unified Soil Classification System).
[2] Atkinson JH, Bransby PL. The mechanics of soils, an introduction to critical state soil mechanic. McGraw-Hill Book Co.; 1977.
[3] Balkaya M, Moore ID, Sağlamer A. Study of nonuniform bedding support because of erosion under cast iron water distribution pipes. J Geotech Geoenviron Eng 2012;138(10):1247–56. https://doi.org/10.1061/(ASCE)GT.1943-5606.0000689.
[4] Beaton JL. and Stratfull RF. Field test for estimating service life of corrugated metal pipe culverts. Proceedings of the 41st Annual Meeting of the Highway Research Board, Washington, D.C., 1962. Vol. 41, pp.255-272.
[5] Billing JR, Green R. Design provisions for dynamic loading of highway bridges. Transp Res Rec 1984;950. http://onlinepubs.trb.org/Onlinepubs/trr/1984/950/950v1-015.pdf.
[6] Bradford SA. The practical handbook of corrosion control in soils. Edmonton, Alberta, Canada: CASTI Publishing Inc; 2000.
[7] Cichocki R, Moore I, Williams K. Steel buried structures: condition of Ontario structures and review of deterioration mechanisms and rehabilitation approaches. Can J Civ Eng 2021;48(2):159–72. https://doi.org/10.1139/cjce-2019-0580.
[8] Institute CSP. 4V6, Corrugated Steel Pipe Institute. Handbook of steel drainage and highway construction products. Cambridge, Ontario, Canada N3H: American Iron and Steel Institute (Canadian Edition); 2010.
[9] CSA-S6, 2014. Canadian Highway Bridge Design Code S6-14 CSA Canadian Standards Association, Canada.
[10] De la Fuente D, Díaz I, Simancas J, Chico B, Morcillo M. Long-term atmospheric corrosion of mild steel. Corros Sci 2011;53(2):604–17. https://doi.org/10.1016/j.corsci.2010.10.007.
[11] Deng L, Cai CS, Barbato M. Reliability-based dynamic load allowance for capacity rating of prestressed concrete girder bridges. J Bridge Eng 2011;16(6):872–80. https://doi.org/10.1061/(ASCE)BE.1943-5592.0000178.
[12] El-Taher M, Moore ID. Finite element study of stability of corroded metal culverts. Transp Res Rec 2008;2050(1):157–66. https://doi.org/10.3141/2050-16.
[13] Elshimi TM, Mak AC, Brachman RWI. and Moore ID. Behaviour of a deep-corrugated large-span box culvert during backfilling. In Pan-American Conference on Teaching and Learning of Geotechnical Engineering, 2011 Pan-Am CGS, Geotechnical Conference. 2011.
[14] Elshimi TM, Moore ID. Modeling the effects of backfilling and soil compaction beside shallow buried pipes. J Pipeline Syst Eng Pract 2013;4(4):04013004. https://doi.org/10.1061/(ASCE)PS.1949-1204.0000136.
[15] Feliu S, Morcillo M, Feliu Jr S. The prediction of atmospheric corrosion from meteorological and pollution parameters—II. Long-term forecasts Corrosion Science 1993;34(3):415–22. https://doi.org/10.1016/0010-938X(93)90113-U.
[16] Giresini L, Puppio ML, Sassu M. Collapse of corrugated metal culvert in Northern Sardinia: analysis and numerical simulations. International Journal of Forensic Engineering 2016;3(1–2):69–85. https://doi.org/10.1504/IJFE.2016.075991.

[17] Hepfner JJ. Statewide corrosivity study on corrugated steel culvert pipe (No. FHWA/MT-01-001/8148). Montana. Department of Transportation. Research, Development and Technology Transfer Program. 2002.
[18] Hibbitt H, Karlsson B. and Sorensen P. Abaqus analysis user's manual version 6.13. Dassault Systèmes Simulia Corp.: Providence, RI, USA; 2013.
[19] Leung C, Meguid MA. An experimental study of the effect of local contact loss on the earth pressure distribution on existing tunnel linings. Tunn Undergr Space Technol 2011;26(1):139–45. https://doi.org/10.1016/j.tust.2010.08.003.
[20] Mai VT. Assessment of Deteriorated Corrugated Steel Culverts. Queen's University; 2013. p. 233p. MSc Thesis.
[21] Mai VT, Hoult N, Moore I. Numerical evaluation of a deeply buried pipe testing facility. Adv Struct Eng 2018;21(16):2571–88. https://doi.org/10.1177/1369433218783769.
[22] McGrath TJ, Selig ET, Webb MC. and Zoladz GV. Pipe interaction with the backfill envelope (No. FHWA-RD-98-191). University of Massachusetts at Amherst. Transportation Center. 1999.
[23] Meegoda JN, Juliano TM, Tang C. Culvert information management system. Transp Res Rec 2009;2108(1):3–12. https://doi.org/10.3141/2108-01.
[24] Meguid MA, Dang HK. The effect of erosion voids on existing tunnel linings. Tunn Undergr Space Technol 2009;24(3):278–86. https://doi.org/10.1016/j.tust.2008.09.002.
[25] Meguid MA, Kamel S. A three-dimensional analysis of the effects of erosion voids on rigid pipes. Tunn Undergr Space Technol 2014;43:276–89. https://doi.org/10.1016/j.tust.2014.05.019.
[26] Menetrey P, Willam KJ. Triaxial failure criterion for concrete and its generalization. Structural Journal 1995;92(3):311–8.
[27] Mikhailov AA, Tidblad J, Kucera V. The classification system of ISO 9223 standard and the dose–response functions assessing the corrosivity of outdoor atmospheres. Prot Met 2004;40(6):541–50. https://doi.org/10.1023/B:PROM.0000049517.14101.68.
[28] Nakhostin E, Kenny S. and Sivathayalan S. Buried corrugated steel culvert failure mechanisms due to environmental deteriorations. In International Conference on Sustainable Infrastructure 2019: Leading Resilient Communities through the 21st Century (pp. 29-40). Reston, VA: American Society of Civil Engineers. 2019, November. https://doi.org/10.1061/9780784482650.004.
[29] Nakhostin E, Kenny S, Sivathayalan S. Numerical performance assessment of buried corrugated metal culvert subject to service load conditions. Can J Civ Eng 2021;48(2):99–114. https://doi.org/10.1139/cjce-2019-0316.
[30] Peter JM, Chapman D, Moore ID, Hoult N. Impact of soil erosion voids on reinforced concrete pipe responses to surface loads. Tunn Undergr Space Technol 2018;82:111–24.
[31] Peter JM, Moore ID. Effects of Erosion Void on Deteriorated Metal Culvert before and after Repair with Grouted Slip Liner. J Pipeline Syst Eng Pract 2019;10(4):04019031. https://doi.org/10.1061/(ASCE)PS.1949-1204.0000399.
[32] Ramberg W. and Osgood WR. Description of stress-strain curves by three parameters. 1943.
[33] Regier C. Investigation of the Failure Mechanisms of Intact and Deteriorated Culverts. Queen's University; 2015. p. 147p. PhD Thesis.
[34] Rubin H, Tokarev D, Rubin E, Schuttrumpf H. Bed Load Erosion Patterns and Their Effect on the Structural Strength of Rigid Pipes Made of Homogeneous Materials. The Open Civil Engineering Journal 2013;7(1):32–49. https://doi.org/10.2174/1874149520130417001.
[35] Walker AC, Williams KA. Strain based design of pipelines. New York, United States: American Society of Mechanical Engineers; 1995.
[36] Wang J, Huang H, Xie X, Bobet A. Void-induced liner deformation and stress redistribution. Tunn Undergr Space Technol 2014;40:263–76. https://doi.org/10.1016/j.tust.2013.10.008.
[37] Wood DM. Soil behaviour and critical state soil mechanics. Cambridge University Press; 1990.
[38] Wriggers P. Finite element algorithms for contact problems. Arch Comput Methods Eng 1995;2(4):1–49. https://doi.org/10.1007/BF02736195.
[39] Xu LY, Cheng YF. Development of a finite element model for simulation and prediction of mechano-electro-chemical effect of pipeline corrosion. Corros Sci 2013;73:150–60. https://doi.org/10.1016/j.corsci.2013.04.004.
[40] Yasuda N, Tsukada K, Asakura T. Elastic solutions for circular tunnel with void behind lining. Tunn Undergr Space Technol 2017;70:274–85. https://doi.org/10.1016/j.tust.2017.08.032.